ACS APPLIED MATERIALS & INTERFACES

Research Article

www.acsami.org

Transparent Luminescent Hyperbranched Epoxy/Carbon Oxide Dot Nanocomposites with Outstanding Toughness and Ductility

Bibekananda De,[†] Brigitte Voit,[‡] and Niranjan Karak*[,†]

[†]Advanced Polymer and Nanomaterial Laboratory, Department of Chemical Sciences, Tezpur University, Napaam 784028, Assam, India

[‡]Leibniz Institute of Polymer Research Dresden, Hohe Strasse 6, D-01069 Dresden, Germany

Supporting Information

ABSTRACT: A luminescent transparent hyperbranched epoxy nanocomposite with previously unachieved outstanding toughness and elasticity has been created by incorporation of a very small amount of carbon oxide nanodots. The nanocomposites of the hyperbranched epoxy with carbon oxide dots at different dose levels (0.1, 0.5, and 1.0 wt %) have been prepared by an *ex situ* solution technique followed by curing with poly(amido-amine) at 100 °C. Different characterizations and evaluations of mechanical and optical properties of the nanocomposites have been performed. The toughness (area under the stress−strain curve) of the pristine system has been improved dramatically by 750% with only 0.5 wt % carbon oxide dots. The tensile strength has been enhanced from 38 to 46 MPa, whereas the elongation at break improved noticeably from 15 to 45%. Excellent adhesive strength combined with transparency and photoluminescent behavior renders these materials highly interesting as functional films in optical devices like light-emitting diodes and UV light detection systems as well as in anticounterfeiting applications.

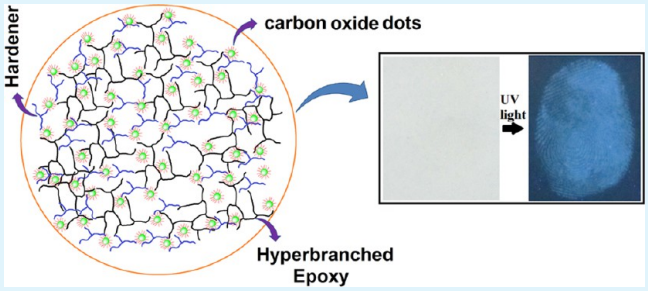

KEYWORDS: *hyperbranched epoxy resin, carbon oxide dot, nanocomposite, toughness, optical properties*

INTRODUCTION

Epoxy resins are widely used for a long time as a matrix in high-performance composite materials. The thermosets of this class of resins attain good mechanical strength, dimensional stability, and chemical resistance, but because of the lack of toughness and, thus, the high brittleness of epoxy resins, many advanced engineering applications cannot be addressed by epoxy-based thermosets.[1−4] Therefore, various concepts have been developed, including blending with flexible polymers to impart the desired toughness and flexibility into these brittle thermosets.[5−10] However, processing difficulties and insufficient improvement in performance still restrict their further commercial exploitation. In this endeavor, recently hyperbranched epoxy resins or the addition of hyperbranched polymeric additives to epoxies received significant attention because of their added advantages like low solution and melt viscosity, high solubility, and high reactivity;[1,11−15] however, it was difficult to achieve the desired material performance of the resulting thermosets.[11] It is pertinent to mention here that in our recent report it has been proven that the proper design of such a hyperbranched epoxy resin with a combination of aromatic and aliphatic moieties can result in a significant improvement in performance.[1] Furthermore, recent studies confirmed the enhancement of many desired properties of a pristine polymer by the formation of suitable nanocomposites using appropriate nanomaterials. In this respect, carbon-based nanomaterials like carbon nanotubes, graphene, etc., are widely used because of their high aspect ratio, their low density, and their outstanding strength and stiffness along with additional functions;[16−19] however, strong van der Waals forces cause the poor dispersion ability of these nanomaterials in the polymer matrix, and thus, they have to be functionalized by often strong oxidizing agents. Further, the transparency of the pristine polymers is also often lost even below 1 wt % loading with these carbon-based nanomaterials. In addition, the potential toxicity of these nanomaterials can cause problems in many applications.

Recently, we have reported the facile preparation of highly polar water-soluble luminescent carbon dots <10 nm in size, which have many oxygen containing groups and are therefore referred better to as carbon oxide dots.[20] Compared to other nanomaterials, they are superior because of their easy availability, high water solubility, compatibility with many polymer matrices, nontoxicity, and high biocompatibility.[20−26] They are mainly applied in biological labeling, optoelectronic devices, etc.[20−26] To the best of our knowledge, there is no report of incorporation of carbon oxide dots into a polymer matrix, although it has strong potential. Here we report, therefore, a simple fabrication of carbon oxide dot-based hyperbranched epoxy nanocomposites to obtain highly tough,

Received: June 24, 2013
Accepted: September 23, 2013
Published: September 23, 2013

Table 1. Performance of the Nanocomposites

parameter	ECD0	ECD0.1	ECD0.5	ECD1.0	DEBA
curing (min) at 100 °C	80 ± 3	60 ± 2	45 ± 1	40 ± 2	75 ± 1
swelling (%) at 25 °C	24 ± 0.5	22 ± 0.8	20 ± 0.9	20 ± 0.6	21 ± 0.4
tensile strength (MPa)	38 ± 1.0	40.7 ± 1.4	46 ± 1.8	42 ± 1.3	38 ± 1.0
elongation at break (%)	15 ± 1	34 ± 1.6	45 ± 1.3	61 ± 1.2	5 ± 0.5
toughness[a]	253 ± 8	982 ± 12	1452 ± 18	1889 ± 19	143 ± 6
impact strength (cm)[b]	>100	>100	>100	>100	65 ± 4.0
scratch hardness (kg)[c]	9.0 ± 0.5	>10.0	>10.0	>10.0	7 ± 0.5
bending diameter (mm)[d]	>1	>1	>1	>1	<4
adhesive strength, W−W (MPa)[e]	2680 ± 12	4691 ± 18	>5678 ± 8	>5686 ± 14	944 ± 8
adhesive strength, M−M (MPa)	2662 ± 9	4272 ± 7	7060 ± 19	9136 ± 26	822 ± 10

[a]Calculated by integrating the area under stress−strain curves. [b]The limit of the impact strength was 100 cm (highest). [c]The limit of the scratch hardness was 10.0 kg (highest). [d]The limit of the mandrel diameter was 1 mm (lowest). [e]In the cases of ECD0.5 and ECD1.0, wood substrates failed.

elastic, and transparent epoxy thermosets for potential advanced material applications, including optical devices. The presence of an aromatic carbonized structure in the carbon oxide dots combined with highly polar surface functional groups can lead to good physicochemical interactions of the hyperbranched epoxy and the hardener. This may offer simultaneous improvement in strength and toughness. Further, the unison of quantum size and good compatibility of carbon oxide dots with the matrix may also result in transparent thermosets, unlike what can be achieved with other carbon-based nanomaterials. In addition, the optical emission in different UV regions of carbon oxide dots of different sizes in the polymer matrix may lead to useful materials for optical devices like light-emitting diodes[27] and UV light detector systems as well as in anticounterfeiting applications.

Therefore, we report for the first time the fabrication, characterization, and evaluation of properties of hyperbranched epoxy/carbon oxide dot nanocomposites as advanced materials for future optical devices with strong potential for commercialization.

EXPERIMENTAL SECTION

Materials. Triethanolamine (Merck, India) was used after vacuum drying. Bisphenol A and epichlorohydrin were purchased from G. S. Chemical (Mumbai, India). Bisphenol A was recrystallized from toluene (Merck, India) before being used. Sodium hydroxide (Rankem, New Delhi, India), ethanol (Merck, India), and poly(amido-amine) hardener (HY840, Ciba Geigy, Mumbai, India; amine equivalent of 5−7 equiv/kg) were used as received without any further purification. Banana (*Musa acuminate*) was collected near the fruits vender from the local market of Assam, India. All other reagents used in this investigation were of reagent grade.

Preparation of Hyperbranched Epoxy Resin. The hyperbranched epoxy resin was prepared by the $A_2 + B_3$ polycondensation reaction of bisphenol A and epichlorohydrin with triethanolamine (20 wt % with respect to bisphenol A) as reported previously.[1] The reaction was conducted at 110 °C for 4 h using aqueous NaOH as the catalyst. The degree of branching of the hyperbranched epoxy was 0.79 (the general structure of the hyperbranched epoxy is given in Figure S1 of the Supporting Information). The epoxy equivalent and hydroxyl value of the hyperbranched epoxy were 358 g/equiv and 102 mg of KOH/g, respectively.

Preparation of Carbon Oxide Dots. The carbon oxide dots were prepared by simple heating of banana juice at 150 °C in a glass bottle as reported previously.[20] The ethanolic solution of the mixture was centrifuged at 960*g* (3000 rpm) for 15 min under ambient conditions to separate the coarse particles. The average size of the spherical carbon oxide dots was 3.5 nm with a narrow size distribution ranging from 1.5 to 4.5 nm (Figure S3a of the Supporting Information).

Preparation of Nanocomposites. The hyperbranched epoxy/carbon oxide dot nanocomposites were prepared by the solution technique. The requisite amount (0.1, 0.5, and 1.0 wt % solid carbon oxide dot) of an ethanolic solution of carbon oxide dots was added to the bulk hyperbranched epoxy polymer, and the mixture was stirred mechanically for 10 h followed by ultrasonication (acoustic power density of 460 W/cm^2) at 60% amplitude and 0.5 cycle for 10 min at room temperature. Then, 50 wt % poly(amido-amine) [the general structure of the poly(amido-amine) is shown in Figure S1 of the Supporting Information] was added to the mixture described above, and the components were mixed homogeneously at room temperature. The mixture was coated on mild glass plates (75 mm × 25 mm × 1.3 mm) for the scratch hardness and tensile test and on steel plates (150 mm × 50 mm × 1.6 mm) for the impact resistance test. The plates were cured at 100 °C for a specified time after being degassed under vacuum for 24 h at room temperature. Then the cured thin films (thickness of 0.3−0.4 mm) were peeled off from the glass plates after their immersion in hot water (70 °C), and the films were dried under vacuum at room temperature. The nanocomposites were named ECD0.1, ECD0.5, and ECD1.0, corresponding to 0.1, 0.5, and 1.0 wt % carbon oxide dots, respectively. The pristine hyperbranched epoxy thermoset without carbon oxide dots was named ECD0.

Characterization. The ultrasonication for the preparation of the nanocomposites was conducted with an ultrasonic processor (UP200S, Hielscher) with a standard sonotrode (trip diameter of 3 mm). The Fourier transform infrared (FTIR) spectra of the hyperbranched epoxy carbon oxide dots and nanocomposites were recorded on a Nicolet FTIR spectrometer (Impact-410) using KBr pellets. The morphology of the nanocomposites was analyzed with a high-resolution transmission electron microscope (TEM) (JEOL, JEMCXII, operating voltage of 200 kV) and a scanning electron microscope (JEOL, JSM-6390 LV). An XRD (X-ray diffraction) (Miniflex, Rigaku Corp.) study was conducted for the carbon oxide dots and the nanocomposite films at room temperature (25 °C) using Cu Kα radiation (λ = 0.154 nm). The scratch hardness evaluation was conducted by a scratch hardness tester (Sheen instrument Ltd.), and the impact strength was evaluated by an impact tester (S. C. Dey Co., Kolkata, India) as per the standard falling weight (ball) method (standard ASTM D 1037). In this test, a weight of 850 g was allowed to fall on the film coated on a mild steel plate from minimal to maximal falling heights. The maximal height was taken as the impact resistance up to which the film was not damaged. The tensile strength and adhesive strength of the nanocomposites were measured with a Universal Testing Machine (UTM, WDW10, Jinan, China) with a 10 kN load cell and crosshead speed of 50 mm/min. The adhesion test of the nanocomposites was conducted on two interfaces of adherents, viz., metal−metal (M−M) and wood−wood (W−W) by the lap-shear test method where the area of the overlapping zone was 25 mm × 25 mm and the thickness of the zone was 0.02−0.03 mm. The lap-shear tensile strength (megapascals) was calculated as the maximal load per unit bonded area, obtained directly from the UTM. All the experiments for the mechanical

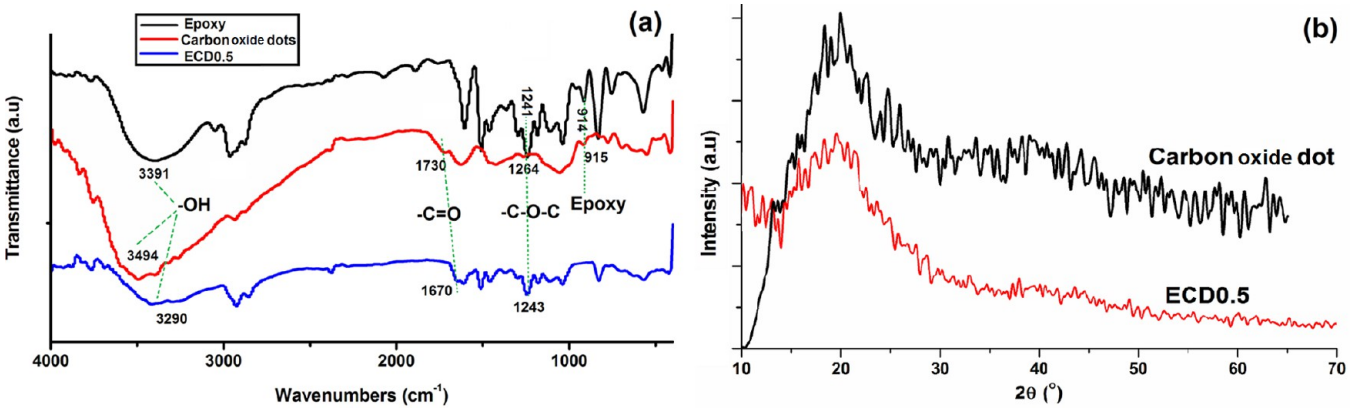

Figure 1. (a) FTIR spectra of hyperbranched epoxy, carbon oxide dot, and nanocomposite (ECD0.5). (b) XRD patterns of carbon oxide dot and nanocomposite (ECD0.5).

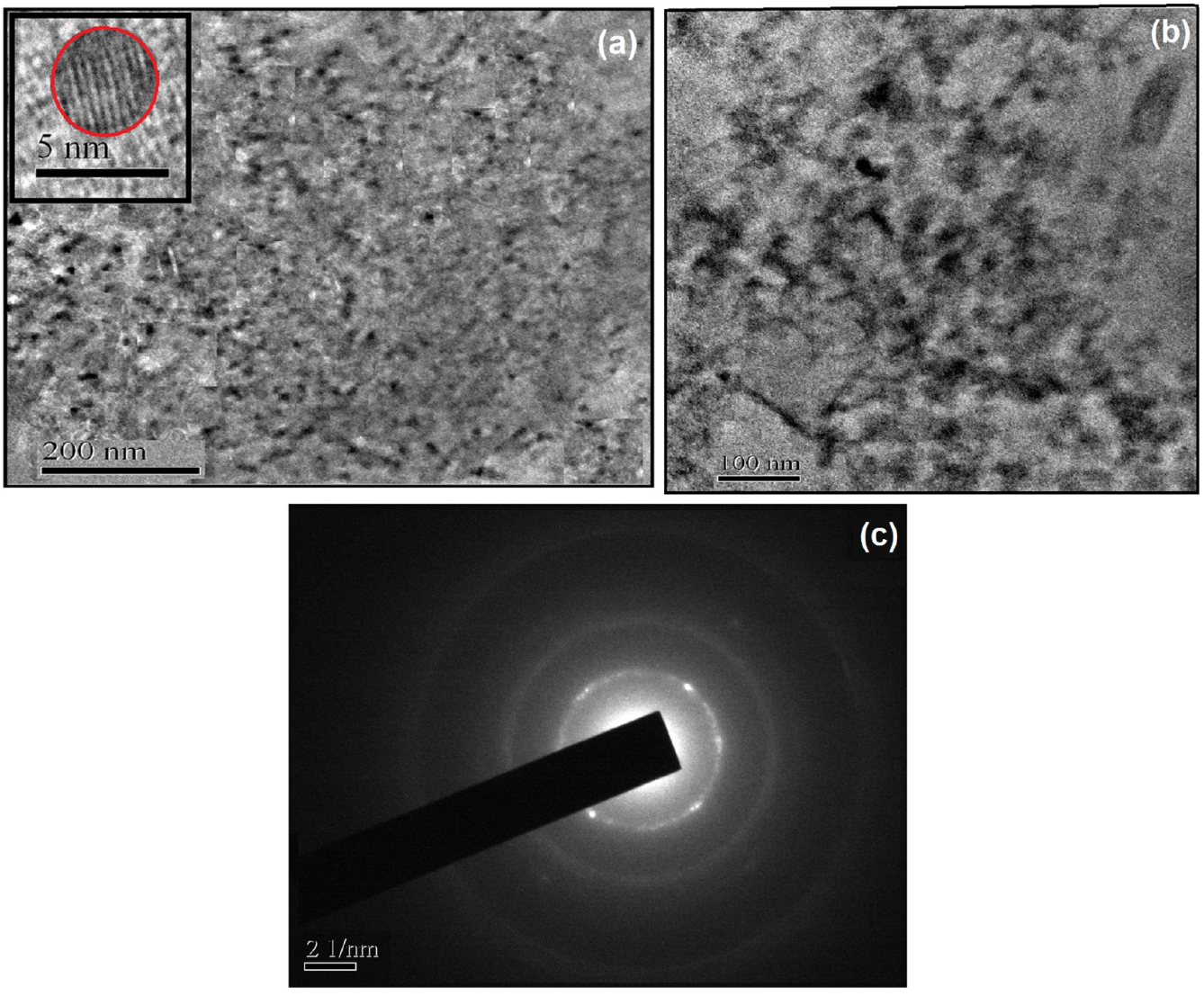

Figure 2. TEM images of (a) ECD0.5 [overview picture and individual integrated carbon oxide nanodot with internal structure (inset)] and (b) ECD1.0. (c) SAED pattern of ECD0.5.

properties were repeated five times, and the average values were taken. UV−visible absorption spectra of the nanocomposite films (thickness of 0.3−0.4 mm) were recorded using a UV spectrometer (U2001, Hitachi, Tokyo, Japan). The percentages of transmittances of the nanocomposites films were calculated from UV−visible absorption spectra. The visual transparency of the nanocomposites was checked by a pen mark covered with the thin thermosetting films (thickness of 0.3−0.4 mm). The optical color emission photos of the nanocomposite films, logos, and fingerprint were recorded in a UV light chamber (Test Master, Kolkata, India). The dilute ethanolic solution

dx.doi.org/10.1021/am402415g | ACS Appl. Mater. Interfaces 2013, 5, 10027−10034

of the nanocomposite (ECD0.5) was used to make a fingerprint on a white paper and dried at 60 °C for 1 h. The photoluminescent spectra were recorded using a photoluminescent setup (model LS 55, Perkin Elemer Singapore PTE Ltd., Singapore) using thin films (0.3−0.4 mm) of the nanocomposites.

RESULTS AND DISCUSSION

Preparation and Characterization of Nanocomposites. The nanocomposites of hyperbranched epoxy and carbon oxide dots were prepared by an *ex situ* solution technique with the help of mechanical shearing and ultrasonication forces. Carbon oxide dots were added only in 0.1, 0.5, and 1.0 wt % based on the epoxy resin. The curing time of the nanocomposites with poly(amido-amine) at 100 °C decreases with an increase in the amount of carbon oxide dots (Table 1). This is due to the presence of a large number of polar functional groups (like hydroxy, epoxy, carbonyl, ether, etc., as revealed by the FTIR spectrum) in carbon oxide dots that took part in the cross-linking reaction (Figure S2 of the Supporting Information). This also resulted in a strong interfacial interaction with the hyperbranched epoxy matrix. In the FTIR spectrum (Figure 1a), for the hyperbranched epoxy polymer, the following characteristic absorption bands (ν_{max}) were observed: 3391 (−OH), 2963 (C−H), 1606 (C═C), 1241 (C−O), 1037 (C−C), and 914 cm^{-1} (oxirane). On the other hand, the bands for the carbon oxide dot were found at 3492 (−OH), 2935 (C−H), 1730 (C═O), 1625 (C═C), 1422 (C−O−C), 1264 (C−O), and 915 cm^{-1} (oxirane). In the FTIR spectrum of the nanocomposite, a broad band for the −OH stretching frequency was observed at 3290 cm^{-1}. This shift compared to that of the pristine polymer is due to the strong interactions and chemical cross-linking of carbon oxide dots with the hyperbranched epoxy polymer and the poly(amido-amine) hardener. The carbonyl peak of the carbon oxide dots (1730 cm^{-1}) was also shifted to 1670 cm^{-1} after the formation of nanocomposites. This occurred because of the formation of amide linkages by the reaction of carboxylic acid and ester groups of the carbon oxide dots with the amino groups of the hardener. The oxirane bands of the hyperbranched epoxy polymer (914 cm^{-1}) and carbon oxide dots (915 cm^{-1}) completely vanished in the nanocomposite because of their participation in chemical cross-linking reactions. The formation of nanocomposites further diminished the crystallinity of the poorly crystalline carbon oxide dots as the intensity of the peak of carbon oxide dots at 21° in XRD (Figure 1b) was found to be decreased. The peak was also broadened and shifted to 18° in the nanocomposites. This is due to the disordered arrangement of the atoms caused by the strong interactions of the polar functional groups of the carbon oxide dots and the polymer matrix. The poor crystallinity of carbon oxide dots, which was further decreased by the formation of nanocomposites, is also confirmed by the selected area electron diffraction (SAED) patterns of carbon oxide dots (Figure S3b of the Supporting Information) and ECD0.5 (Figure 2c). An excellent dispersion of carbon oxide dots in the polymer matrix was supported by the TEM micrograph (Figure 2a) of ECD0.5 showing the carbon oxide dots are separated well in the matrix without aggregation. The fine dispersion of the carbon oxide dots is due to the chemical binding to the polymer matrix through their large number of functional surface groups during the curing reaction preventing agglomeration. The internal spacing of the carbon oxide dots was increased after the formation of nanocomposites as shown in the inset of the TEM image. A tendency toward aggregation of carbon oxide dots in the hyperbranched epoxy matrix was observed in the TEM image (Figure 2b) for ECD1.0. Here we speculate that at higher carbon oxide dot concentrations the large number of polar functional surface groups may also favor interactions of the nanodots, assuming that at this concentration not all functional groups are used up in chemical binding reactions to the polymer matrix.

Mechanical Properties of Nanocomposites. Mechanical properties like tensile strength, elongation at break, toughness, impact resistance, scratch hardness, and bending of the pristine hyperbranched epoxy and the nanocomposites are listed in Table 1. In this table, the mechanical properties of a commercial diglycidyl ether of bisphenol A (DEBA)-based epoxy thermoset cured with the same poly(amido-amine) at 50 wt % are also given. From the results, we found that the hyperbranched epoxy thermoset exhibited significantly better performance than the DEBA. However, the elongation at break and the toughness of the hyperbranched epoxide were dramatically further enhanced by factors of 5 and 8, respectively, after the formation of nanocomposites even at very low weight loads (maximum of 1.0 wt %) of the carbon oxide dots. The tensile strength and scratch hardness of the pristine epoxy were also improved by the formation of the nanocomposites. The tensile strength increases with an increase in carbon oxide dot content as shown in Figure S4 of the Supporting Information; this is also evident from the stress−strain profiles (Figure 3). However, the tensile strength of

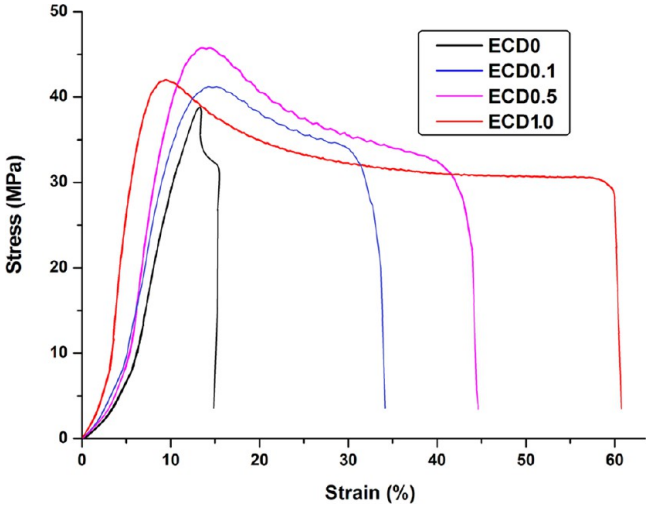

Figure 3. Stress−strain profiles of a hyperbranched epoxy thermoset (ECD0) and the corresponding nanocomposites.

ECD1.0 was lower than that of ECD0.5. This might be due to some aggregation of the carbon oxide dots in the polymer matrix as shown in the TEM image of ECD1.0 (Figure 2b). The nanocomposites also exhibited high impact resistance and flexibility. Because both the pristine hyperbranched epoxy thermoset and the nanocomposites reached the measurement limits of the instruments for impact resistance (100 cm), flexibility evaluation (1 mm), and scratch resistance (10.0 kg), the enhancement of these values by adding the carbon oxide dots could not be quantified, but clearly, these results indicate a dramatic enhancement of toughness of the hyperbranched epoxy thermosets by the incorporation of a very small amount of carbon oxide dots. The stress−strain profiles (Figure 3a) also

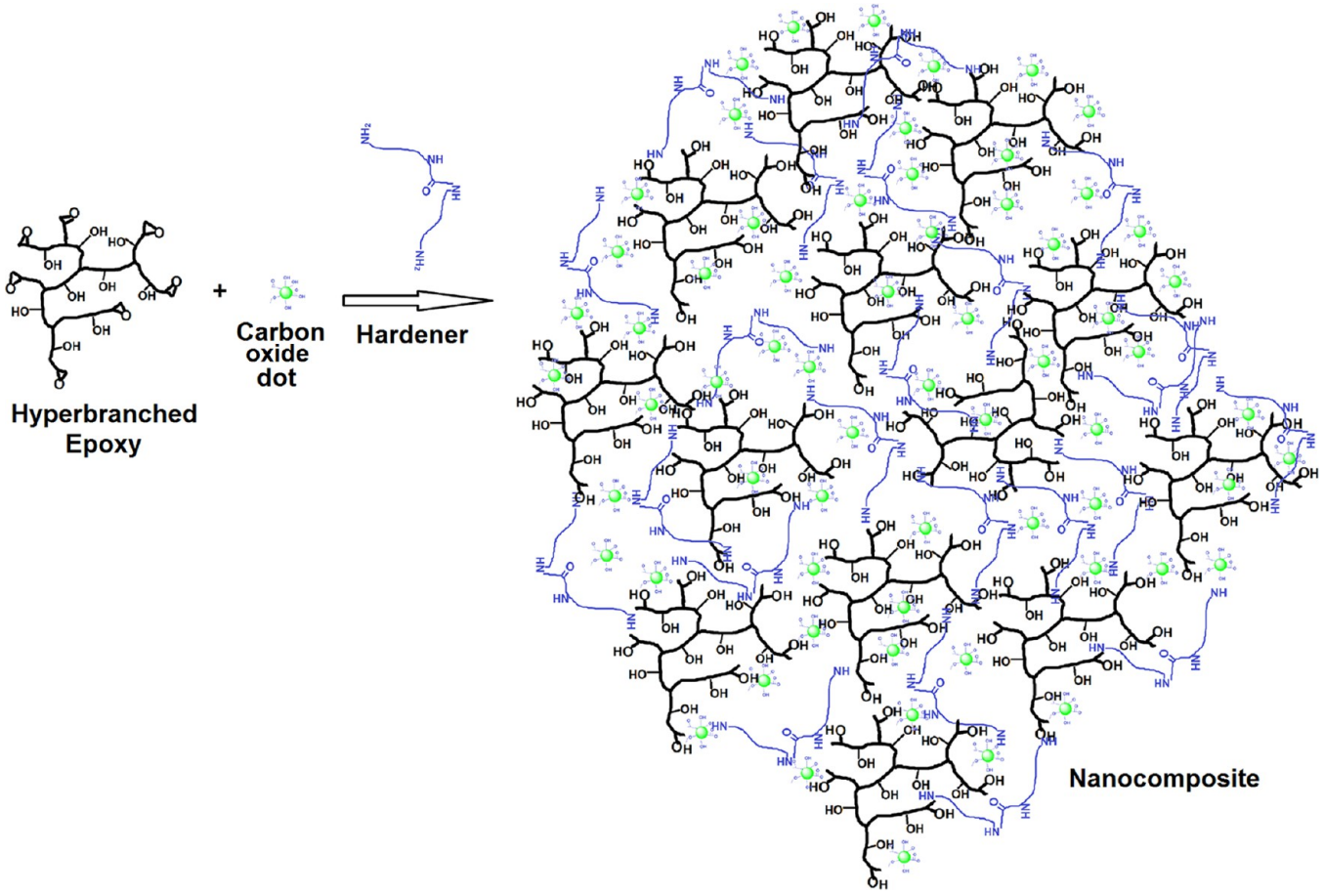

Figure 4. Different physicochemical interactions of carbon oxide dots with hyperbranched epoxy and poly(amido-amine) hardener.

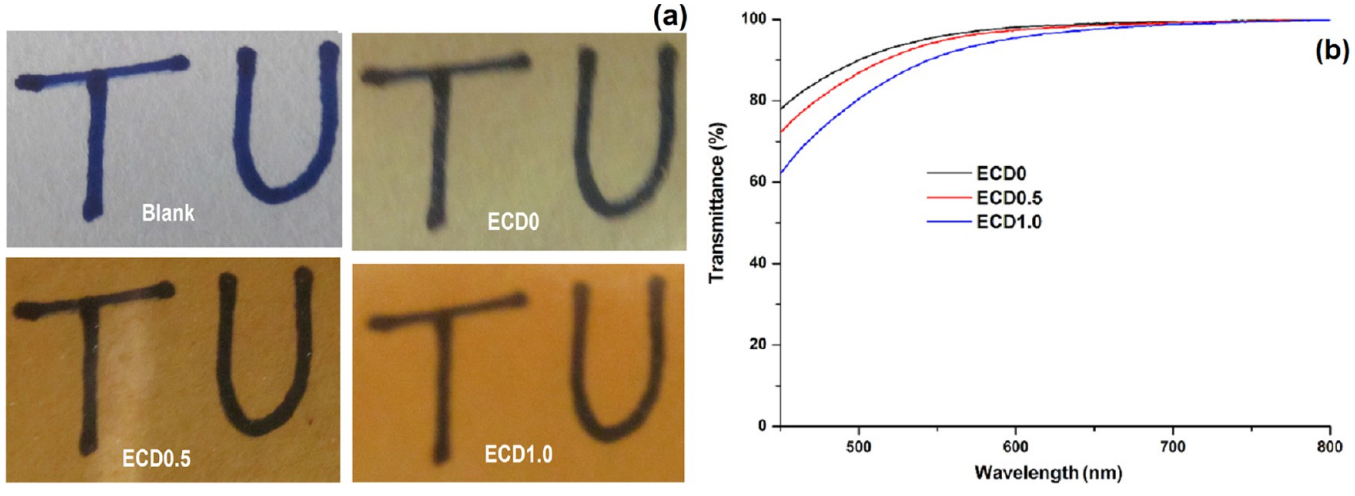

Figure 5. (a) Photos for transparency and (b) visible light transmittance (%) of pristine epoxy and nanocomposite films.

revealed an up to 500% improvement in the elasticity of the epoxy thermoset by the formation of nanocomposites. This simultaneous improvement in the strength, toughness, and flexibility of the hyperbranched epoxy is a highly commendable achievement. We relate this to the presence of the aromatic carbonized core structure combined with a large number of polar surface functional groups in the carbon oxide dots. This provides on one hand a strong and stiff nanomaterial, which enhances the mechanical properties of the polymer matrix, and on the other a very strong physicochemical interaction between the nano dots and the matrix, which is further enhanced by the very small size of the carbon oxide dots resulting in a huge surface area. The polar functional groups (like hydroxy, epoxy, carbonyl, ether, etc.) of the carbon oxide dots take part in the physical and chemical cross-linking reactions with the hyperbranched epoxy resin and the hardener as shown in Figure 4. The strong interfacial interaction of the carbon oxide dots with the matrix helps to enhance the rigidity, as reflected by the enhancement of strength. All these combined effects enhance

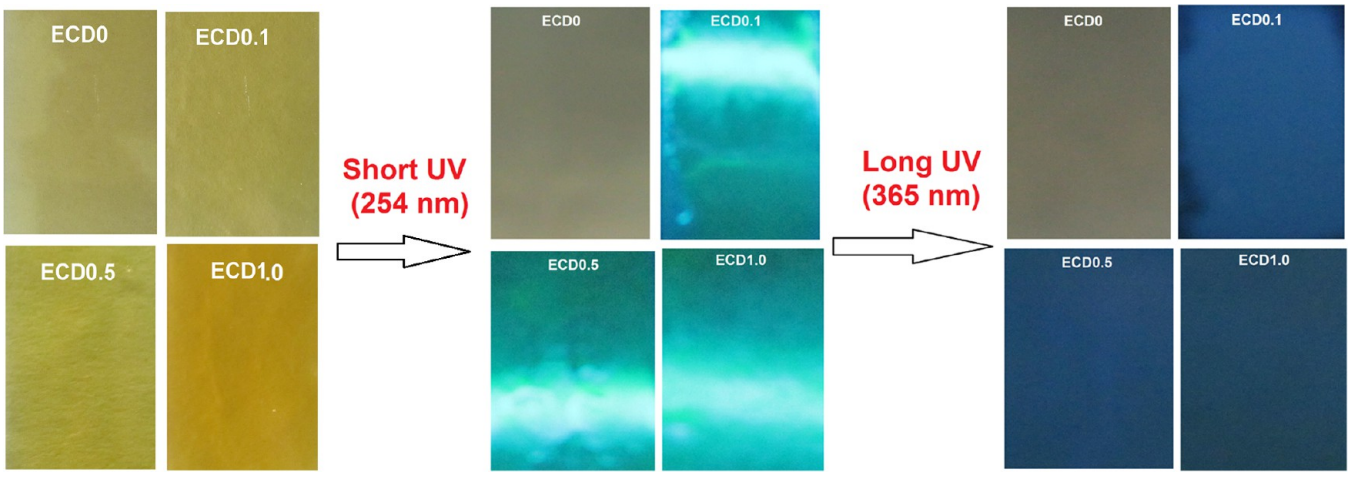

Figure 6. Photos of hyperbranched epoxy thermoset and nanocomposite films at visible, short UV, and long UV (from left to right) regions.

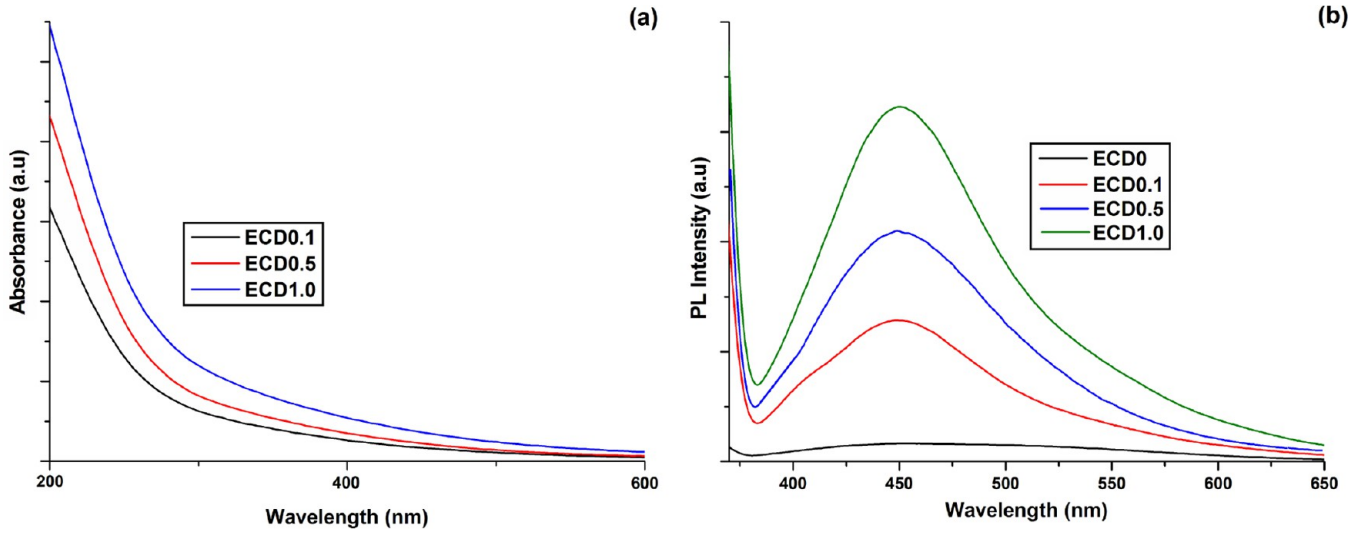

Figure 7. (a) UV and (b) PL spectra of the nanocomposites.

the overall performance, including the tensile strength, elongation at break, and toughness of the thermoset.

Lap-Shear Tensile Adhesive Strength of Nanocomposites. Lap-shear tests revealed >2- and >3-fold enhancements of adhesive strength for wood and metal substrates, respectively, by the incorporation of only 1.0 wt % carbon oxide dots into the hyperbranched epoxy thermoset (Table 1). This is due to the presence of polar functionalities in the nanocomposites that allows for strong interactions and physical interlocking with the substrates, and the number of these interactions increases with an increase in the amount of carbon oxide dots in the thermoset. In the case of ECD0.5 as well as ECD1.0, substrate failure was observed for wood, and thus, the nanocomposites exhibited adhesive strength even greater than the values reported in Table 1. The different polar functional groups of the cellulosic wood substrate strongly interact with the polar functional groups present in the hyperbranched epoxy polymer, the carbon oxide dots, and the hardener. For the metal substrate, however, strong physical interlocking with the hyperbranched epoxy and the different functional groups of carbon oxide dots is the main reason for the high adhesive strength. The strong physical interlocking is due to the easy diffusion of weakly viscous hyperbranched epoxy and hardener along with the spherical fine particles of carbon oxide dots into the surface structure of the metal substrate.

Optical Properties of Nanocomposites. Optical properties like the transparency and luminescence of carbon oxide dot-based polymer nanocomposites are not only interesting but also unique characteristics. These characteristics are difficult to achieve with other carbon-based nanocomposites. The transparency of the cured hyperbranched epoxy resins is not much affected after formation of nanocomposites with carbon oxide dots as can be seen for ECD0, ECD0.5, and ECD1.0 in Figure 5a. The retention of high transparency in the nanocomposites is due to the quantum size (<10 nm) of the carbon oxide dots and the high dispersion quality preserving their nanoscale size in the thermoset due to the chemical cross-linking with the hyperbranched epoxide and the hardener. The percent of transmittance of visible light of the nanocomposite films slightly decreased at shorter wavelengths, as shown in Figure 5b, due to absorption of the light source by the carbon oxide dots in the shorter wavelength of visible light as shown in an earlier study.[20] The optical colors of the nanocomposites in the visible, short UV (254 nm), and long UV (365 nm) regions are shown in the Figure 6. The brown color of the nanocomposite in the visible range was changed to bluish green by illumination with

the short UV light and to dark blue with long UV light. The green and blue color emissions of the nanocomposites are due to the corresponding band gaps of carbon oxide quantum dots at the two excitation wavelengths. The change in color at different wavelengths of UV light is due to the presence of different sizes of carbon oxide dots in the nanocomposites (the size distribution of carbon oxide dots is shown in the TEM image of the carbon oxide dot in Figure S3a of the Supporting Information). The smaller carbon oxide dots are excited in the short UV region, and the larger carbon oxide dots are excited in the long UV region.[20] The maximal optical absorption of the nanocomposites was observed in the UV region, but it extends to the visible range with lower absorption (Figure 7a). This is due to the n−π^* transition of the C═O band and the $\pi-\pi^*$ transition of the conjugated C═C band. The classic signature of the carbon oxide dot is a photoluminescent (PL) behavior that is the most fascinating property of carbon oxide dots from the application point of view. This PL behavior is due to the quantum size of the carbon oxide dot that results in a large band gap due to the quantum confinement effect. In the PL study of the nanocomposites, a strong emission peak located at 450 nm was observed upon excitation at 360 nm (Figure 7b). The intensity of the PL spectra sharply increased with an increase in the carbon oxide dot content. This is due to the fact that the PL intensity depends on the number of particles excited at a particular wavelength.[20] As the number of particles increases with ane increase in the concentration of carbon oxide dot in the nanocomposites, ECD1.0 shows the highest PL intensity.

Applications in Anticounterfeiting. The prepared nanocomposites not only are useful as high-performance advanced materials but also can be used for multifunctional anticounterfeiting applications. As the nanocomposites were soluble in different solvents and can even form a stable emulsion in water before curing, so can the dilute solution or an emulsion of the nanocomposites be used for anticounterfeiting of different delicate designs, including logos and fingerprints. The fingerprint was colorless under visible light but resulted in a fluorescent color under exposure to 365 nm UV light (Figure 8). It is pertinent to mention here that the same utility can also be achieved by using different inorganic semiconductor quantum dots or organic dyes, but in this case, the presence of large numbers of polar functional groups both in the matrix and in nanomaterials offers a strong interaction with the substrate of interest. Further, the thermoset also provides water proofing characteristics in addition to strengthening of the substrate. The study showed that the strength of a cellulosic substrate increased up to 3-fold after application of this thermoset. Thus, this material has multiple advantages in anticounterfeiting applications.

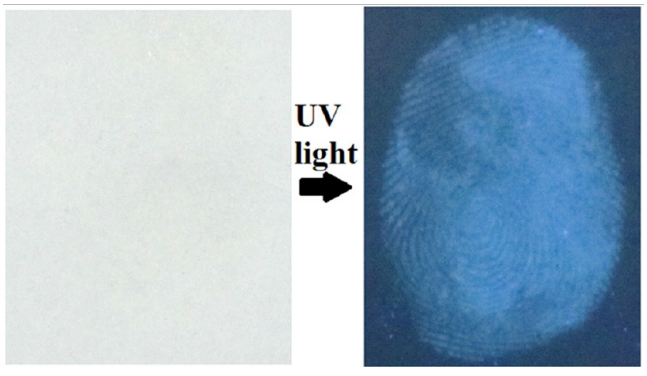

Figure 8. Luminescent photo of a fingerprint under UV exposure at 365 nm.

CONCLUSIONS

In summary we demonstrated for the first time an exceptionally tough, elastic, transparent, and flexible hyperbranched epoxy thermosetting nanocomposite with interesting optical properties by incorporation of a very small amount of carbon oxide dots (<1 wt %). This may open up a new avenue for epoxy thermosets as functional nanocomposite films in advanced optical applications. The high adhesive strength of these thermosetting nanocomposites combined with their advanced properties significantly broadens the application range in advanced technologies. This huge nano effect achieved with the carbon oxide nano dots might be transferred to other matrix polymers when one tunes interface interactions. The emission in different UV regions may be useful in optical devices like light-emitting diodes and UV light detection systems as well as in multifunctional anticounterfeiting applications.

ASSOCIATED CONTENT

Supporting Information

General structure of the hyperbranched epoxy and poly(amidoamine), curing reaction of carbon oxide dots with the hyperbranched epoxy and hardener, a TEM image with size distribution and SAED pattern of the carbon oxide dot, and variations of tensile strength and elongation at break of the nanocomposites. This material is available free of charge via the Internet at http://pubs.acs.org.

AUTHOR INFORMATION

Corresponding Author

*Advanced Polymer and Nanomaterial Laboratory, Department of Chemical Sciences, Tezpur University, Napaam 784028, Assam, India. E-mail: karakniranjan@yahoo.com.

Notes

The authors declare no competing financial interest.

ACKNOWLEDGMENTS

We express our gratitude to SAP (UGC), India, for Grant F.3-30/2009 (SAPII) and the FIST program-2009 (DST), India, for Grant SR/FST/CSI-203/209/1 (May 6, 2010) for financial assistance. SAIF of NEHU, Shillong is gratefully acknowledged for TEM imaging. We are express our thanks to the NRB for financial assistance through Grant DNRD/05/4003/NRB/251 (February 29, 2012).

REFERENCES

(1) De, B.; Karak, N. *J. Mater. Chem. A* **2013**, *1*, 348−353.
(2) Karak, N. *Fundamentals of Polymers: Raw Materials to Applications*; PHI Learning Pvt. Ltd.: New Delhi, 2009.
(3) Lee, H.; Neville, K. *Handbook of Epoxy Resins*; McGraw-Hill: New York, 1967.
(4) Barua, S.; Dutta, G.; Karak, N. *Chem. Eng. Sci.* **2013**, *95*, 138−147.
(5) Qi, G.; Zhang, X.; Li, B.; Song, Z.; Qiao, J. *Polym. Chem.* **2011**, *2*, 1271−1274.
(6) Ratna, D.; Banthia, A. K. *Polym. Int.* **2000**, *49*, 281−287.
(7) Chikhi, N.; Fellahi, S.; Bakar, M. *Eur. Polym. J.* **2002**, *38*, 251−264.

(8) Ivanova, K. I.; Pethrick, R. A.; Affrossman, S. *Polymer* **2000**, *41*, 6787−6796.
(9) Shin, S. M.; Shin, D. K.; Lee, D. C. *J. Appl. Polym. Sci.* **2000**, *78*, 2464−2473.
(10) Fu, J. F.; Shi, L. Y.; Yuan, S.; Zhong, Q. D.; Zhang, D. S.; Chen, Y.; Wu, J. *Polym. Adv. Technol.* **2008**, *19*, 1597−1607.
(11) Zhang, D.; Jia, D. *J. Appl. Polym. Sci.* **2006**, *101*, 2504−2511.
(12) Ratna, D.; Varley, R.; Simon, G. P. *J. Appl. Polym. Sci.* **2003**, *89*, 2339−2345.
(13) Wang, X.; Feast, W. J. *Chin. J. Polym. Sci.* **2002**, *20*, 585−590.
(14) Sangermano, M.; Priola, A.; Malucelli, G.; Bongiovanni, R.; Quaglia, A.; Voit, B.; Ziemer, A. *Macromol. Mater. Eng.* **2004**, *289*, 442−446.
(15) Morell, M.; Erber, M.; Ramis, X.; Ferrando, F.; Voit, B.; Serra, A. *Eur. Polym. J.* **2010**, *46*, 1498−1509.
(16) Lahiri, D.; Rouzaud, F.; Namin, S.; Keshri, A. K.; Valdes, J. J.; Kos, L.; Tsoukias, N.; Agarwal, A. *ACS Appl. Mater. Interfaces* **2009**, *1*, 2470−2476.
(17) Sun, D.; Chu, C. C.; Sue, H. J. *Chem. Mater.* **2010**, *22*, 3773−3778.
(18) Rafiee, M. A.; Rafiee, J.; Wang, Z.; Song, H.; Yu, Z. Z.; Koratkar, N. *ACS Nano* **2009**, *3*, 3884−3890.
(19) Terrones, M.; Martin, O.; Gonzalez, M.; Pozuelo, J.; Serrano, B.; Cabanelas, J. C.; Diaz, S. M. V.; Baselga, J. *Adv. Mater.* **2011**, *23*, 5302−5310.
(20) De, B.; Karak, N. *RSC Adv.* **2013**, *3*, 8286−8290.
(21) Jia, X.; Li, J.; Wang, E. *Nanoscale* **2012**, *4*, 5572−5575.
(22) Li, Q.; Ohulchanskyy, T. Y.; Liu, R.; Koynov, K.; Wu, D.; Best, A.; Kumar, R.; Bonoiu, A.; Prasad, P. N. *J. Phys. Chem. C* **2010**, *114*, 12062−12068.
(23) Goh, E. J.; Kim, K. S.; Kim, Y. R.; Jung, H. S.; Beack, S.; Kong, W. H.; Scarcelli, G.; Yun, S. H.; Hahn, S. K. *Biomacromolecules* **2012**, *13*, 2554−2561.
(24) Yang, S. T.; Cao, L.; Luo, P. G.; Lu, F.; Wang, X.; Wang, H.; Meziani, M. J.; Liu, Y.; Qi, G.; Sun, Y. P. *J. Am. Chem. Soc.* **2009**, *131*, 11308−11309.
(25) Sun, Y. P.; Zhou, B.; Lin, Y.; Wang, W.; Fernando, K. A. S.; Pathak, P.; Meziani, M. J.; Harruff, B. A.; Wang, X.; Wang, H.; Luo, P. G.; Yang, H.; Kose, M. E.; Chen, B.; Veca, L. M.; Xie, S. Y. *J. Am. Chem. Soc.* **2006**, *128*, 7756−7757.
(26) Li, H.; Kang, Z.; Liu, Y.; Lee, S. T. *J. Mater. Chem.* **2012**, *22*, 24230−24253.
(27) Zou, W.; Du, Z.; Lee, H.; Zhang, C. *J. Mater. Chem.* **2011**, *21*, 13276−13282.